ISSN 2176-5480

22nd International Congress of Mechanical Engineering (COBEM 2013)
November 3-7, 2013, Ribeirão Preto, SP, Brazil

THE LATTICE-BOLTZMANN METHOD FOR DETERMINING THE DRAG COEFFICIENT

Diego Bonkowski de La Sierra Audiffred
Fabiano G. Wolf
Universidade Federal de Santa Catarina
Campus Joinville
Rua Presidente Prudente de Moraes, 406
Bairro Santo Antônio
Joinville - SC - Brasil
89218-000
lasierra_diego@yahoo.com.br, fabiano.wolf@ufsc.br

Abstract. *The determination of drag coefficient has a great importance for aerospace industries and there are basically two effective methods to determine it, first one is by performing experiments in wind tunnels, the second one is by the use of computational methods. The latter tends to be much cheaper than the former. However, it is required that the channel where the body is immersed be significantly larger than the body itself to avoid wall interference effects, which increases the computational cost. Therefore, the objective of this study is to use the Lattice-Boltzmann method (LBM) to understand the influence of the domain size in the results of the computed drag and to find a way to predict drag coefficient over a body by using a much smaller simulation domain than the one usually would be necessary. For this, a two dimensional flow has been considered under low Reynolds number. It has been tested a flow over a cylinder for an easier comparison with experiments. As a result, it was possible to see that performing a couple of computational simulations in some relatively small geometries it is possible to predict with good precision the drag coefficient due its linear behavior with respect to the domain size.*

Keywords: *drag coefficient, cylinder, Lattice-Boltzmann method, length effects.*

1. INTRODUCTION

The determination of aerodynamics forces acting on a body is not just important for aerospace and aviation industries, but for many others as well, such as automotive industry and even for some companies related to sporting goods.

The aerodynamic drag and lift forces on an object depends on several factors, including the shape, size, and flow conditions. All of these factors are related to the value of the drag and lift given by the following equations (NASA, 2013; Houghton and Carpenter, 2003):

$$F_D = \frac{1}{2}\rho V^2 S C_D, \tag{1}$$

$$F_L = \frac{1}{2}\rho V^2 S C_{L,} \tag{2}$$

Where $\rho V^2/2$ corresponds to the dynamic pressure of the free-stream flow, S is the cross-sectional area, C_D and C_L are respectively the drag and lift coefficient, they both are dimensionless number that characterizes all of the complex factors affecting the drag and lift forces, and these forces are proportional to these coefficients. They can be determined experimentally using a model in a wind tunnel. However it tends to be very expensive, so an alternative method to do it is through computational simulations.

Related to computational methods of flow simulations, there is the Lattice-Boltzmann method, it is a relatively new computational method to solve problems involving fluid dynamics and it is increasingly attracting a great number of researches from different areas, mainly because it can easily represents many complex physical phenomena.

Determining the aerodynamics forces on a body are not really a challenge using the Lattice-Boltzmann method. However, to receive accurate results from the simulations it is necessary that the channel where the body is immersed be much greater than the body itself, just like in wind tunnels experiments. In addition there is a limitation in the speed values of the fluid by using this method. Therefore, it is easy to see that simulating, for instance, a flow with a high number of Reynolds can take a long time even for flow simulations over simple geometries. That is why the present paper study a different way of determining these important aerodynamic coefficients commented above, which implies in run some simulations using relatively small channels and so predict how would be the result using a channel of infinity dimension. As mentioned above, to compare with experimental results, it will be simulated a flow around a cylinder to determine the drag and lift coefficient, but basically only the drag will be analyzed since there is no lift due to the flow over a cylinder with no spin.

ISSN 2176-5480

2. FLOW AROUND A CYLINDER

Flow over a cylinder is a fluid mechanics problem of practical importance. According to Devenport (2013), a two-dimensional flow around a cylinder is one of the most studied of aerodynamics. The flow pattern and the drag on a cylinder are mainly characterized as functions of the Reynolds number which can be calculated as indicated by Eq. (3).

$$Re = \frac{DU}{\upsilon}, \tag{3}$$

in which D is the diameter of the cylinder, U is the undisturbed free-stream velocity and υ is the kinematic viscosity.

Houghton and Carpenter (2003) present the following description for the flow pattern around a cylinder considering low Reynolds number:

At very low Reynolds number, Re<<1, the flow behaves as if it were purely viscous with negligible inertia, in this case the streamlines are completely symmetrical, as depicted in Fig. 1a. This kind of flow is known as creeping or Stokes flow. The flow changes a lot as the Reynolds number is increased.

When Re exceeds a value of approximately 5, the flow pattern changes, it separates from the cylinder surface to form a closed wake of recirculating flow. This wake continually grows in length as Re is increased by 5 up to about 41, it is shown in Fig. 1b. The flow pattern is symmetrical about the horizontal axis and it does not change with time, so it is a steady flow.

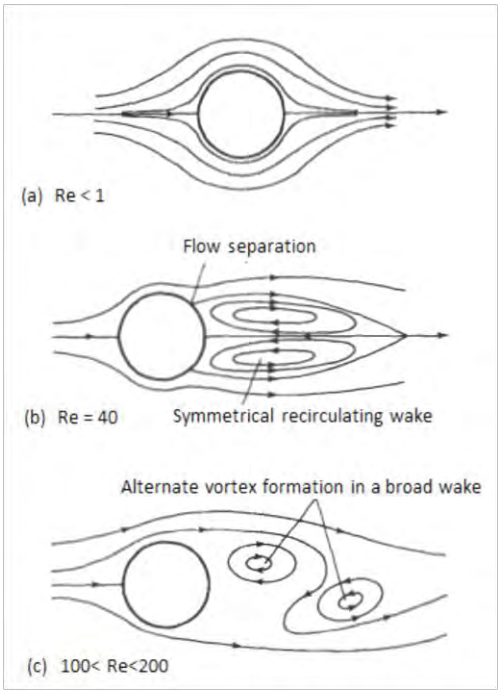

Figure 1. Regimes of flow around a smooth, circular cylinder in steady current

When Re exceeds a value of about 41 another profound change occurs, it is no more a steady flow. What happens is similar to the early stages of laminar-turbulent transition, in that the steady recirculating wake flow becomes unstable to small disturbances. In this case, though, the small disturbances develop as vortices rather than waves. Also in this case, the small disturbances do not develop into turbulent flow, but rather a steady laminar wake develops into an unsteady, but still stable, laminar wake. The vortices are generated periodically on alternate sides of the horizontal axis through the wake and the center of the cylinder, as depicted in figure 1c. In this way, a row of vortices are formed, this vortex row persists for a very considerable distance downstream. This phenomenon is called the Karman vortex street, first explained theoretically by von Kármán. It happened in the first decade of the twentieth century.

For Reynolds numbers between above 40 and about 100 the vortex street develops from amplified disturbances in the wake.

During the formation of any single vortex while it is bound to the cylinder, an increasing circulation will exist about the cylinder, as consequence there will be a lift force generation. With the development of each successive vortex this force will change sign, so it will exist an alternating transverse force on the cylinder at the same frequency as the vortex shedding.

ISSN 2176-5480

There is a relationship between the Reynolds number and a dimensionless parameter involving the shedding frequency. This parameter, known as the Strouhal number, is defined by the expression

$$St = \frac{f_v D}{U}, \tag{4}$$

in which f_v is the vortex-shedding frequency. But this is not the object of study of this paper and to study the characteristics of the flow over a cylinder for Reynolds higher than 100 is not either.

Some authors consider some values for the flow pattern changes slightly different from those presented above. For instance, according to Homann (1936), an experiment of a flow around a circular cylinder results in the flow pattern presented in Fig. 2.

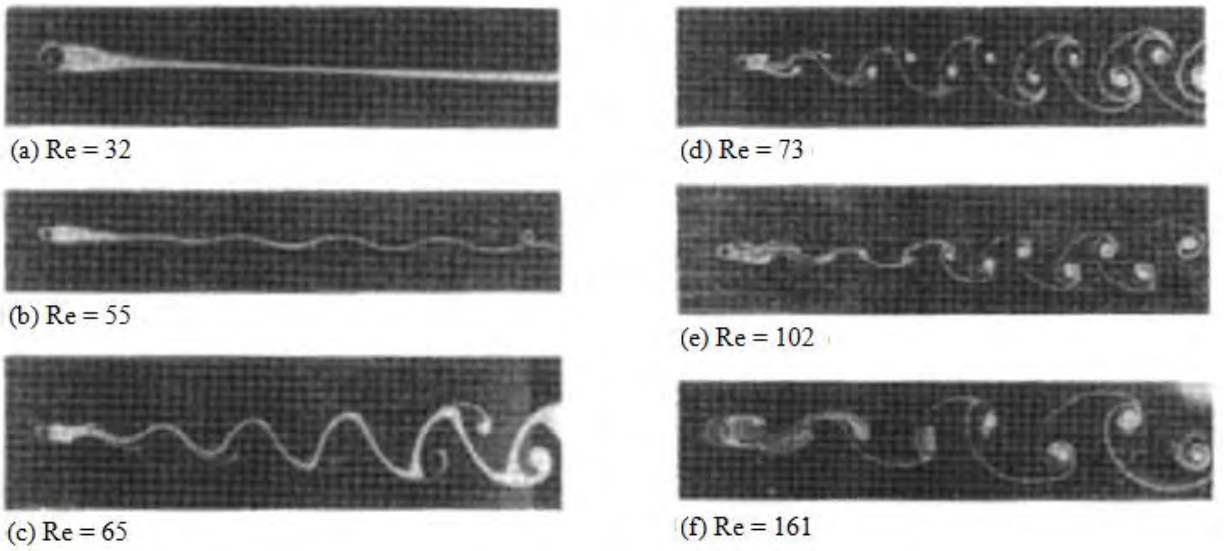

Figure 2. Appearance of vortex shedding behind a circular cylinder.

2.1 Lattice-Boltmann model

The Lattice Boltzmann Method is a mesoscopic approach for the description of a mechanical system of particles. These particles are seen as fictitious ensemble of particles in a discrete lattice domain. Historically, the Boltzmann model originated from the lattice gas automata (Frisch et al., 1986; Wolfram, 1986). It came from the necessity to eliminate some problems as statistic noise that is a result of the Boolean variables use for the description of macroscopic properties, and some others non-physics effects as the explicit dependency of the velocity in the state equation (Rothman e Zaleski, 1997).

One of the most expressive results of this method is the fact of it recover the following governing equations for incompressible flow (Qian et al., 1992; Chen et al., 1992):

$$\nabla \cdot \boldsymbol{u} = 0, \tag{5}$$

$$\frac{\partial \mathbf{u}}{\partial \mathrm{t}} + \mathbf{u} \cdot \nabla \boldsymbol{u} = \frac{\nabla P}{\rho} + \upsilon \nabla^2 \boldsymbol{u}, \tag{6}$$

where **u**, P, ρ e υ represent the velocity of the fluid, pressure, density and kinematic viscosity, respectively. The above equations represent the continuity equation and the Navier-Stokes equation corresponding to mass conservation and momentum conservation.

Considering a three dimensional analysis, the lattice Boltzmann method can use a cubic lattice together with 19 discrete velocities connecting lattice sites known as D3Q19 model as illustrated in Fig. 3a. A corresponding model for two dimensions involves a square lattice with 9 velocities which is known as D2Q9 model as depicted in Fig. 3b.

ISSN 2176-5480

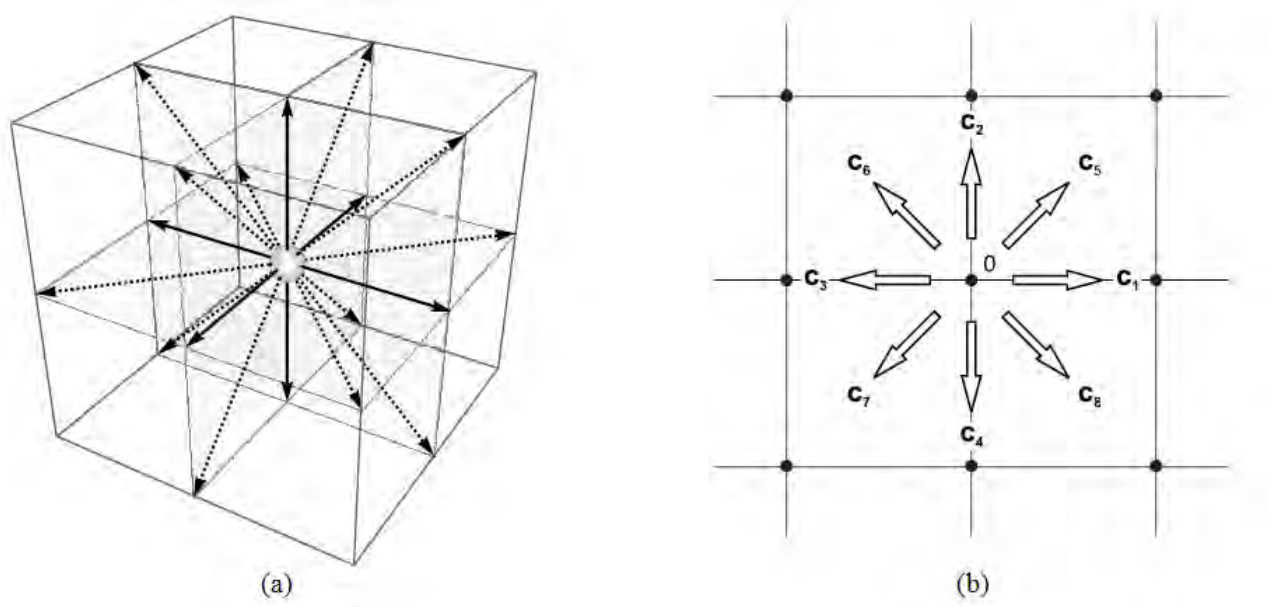

Figure 3. Lattices models used in tridimensional and bidimensional simulations: (a) D3Q19 model; (b) D2Q9 model.

To this square lattice is incorporated a single-particle distribution function. This function can be thought of as a typical histogram representing a frequency of occurrence.

So, the macroscopic velocity **u** is an average of the microscopic velocities **c***a* weighted by the directional densities *fa* as shown below

$$\boldsymbol{u} = \frac{1}{\rho}\sum_{a=0}^{8} f_a\, \boldsymbol{c}_a, \tag{7}$$

where the macroscopic density ρ of the fluid is calculated as indicated below:

$$\rho = \sum_{i=0}^{8} f_i. \tag{8}$$

And the macroscopic pressure is calculated as follows

$$P = c_s^2 \sum_{i=0}^{8} f_i = c_s^2 \rho, \tag{9}$$

where c_s is the speed of sound for the lattice Boltzmann model, it weighs $1/\sqrt{3}$, so the pressure can be calculated just by dividing the density by three.

The streaming and collision of the particles is done via the distribution function. It is used the Bhatnagar-Gross-Krook (BGK) approximation for collision which is the simplest approach. And it can be described like this:

$$f_a(x + \boldsymbol{c}_a \Delta t, t + \Delta t) = f_a(x,t) - \frac{\left[f_a(x,t) - f_a^{eq}(x,t)\right]}{\tau} \tag{10}$$

where $f_a(x + \boldsymbol{c}_a \Delta t, t + \Delta t) = f_a(x,t)$ is the streaming part and $\left[f_a(x,t) - f_a^{eq}(x,t)\right]/\tau$ is the collision term. However, with the presence of solid boundaries these parts must be written separately due to the bounce back boundary condition. Collision of the fluid particles is considered as a relaxation towards a local equilibrium. For the D2Q9 model the equilibrium distribution function feq can be written as

$$f_a^{eq}(\boldsymbol{x}) = w_a \rho(\boldsymbol{x}) \left[1 + 3\frac{\boldsymbol{e}_a \cdot \boldsymbol{u}}{c^2} + \frac{9}{2}\frac{(\boldsymbol{e}_a \cdot \boldsymbol{u})^2}{c^4} - \frac{3}{2}\frac{\boldsymbol{u}^2}{c^2}\right] \tag{11}$$

ISSN 2176-5480

where the weights *wa* are 4/9 for the rest particles ($a = 0$), 1/9 for $a = 1, 2, 3, 4$, and 1/36 for $a = 5, 6, 7, 8$, and c is the basic speed on the lattice (Sukop and Thorne, 2005). The values of a is related to the directions indicated above in Fig. 3b.

For the drag coefficient determination it has been evaluated the momentum of the fluid before and after a collision with a solid boundary. That way the total aerodynamic force can be calculated as follows (Surmas et al., 2004)

$$\boldsymbol{F} = \sum_{\Gamma} \sum_{i} [f_{-i}(\boldsymbol{X}_{\Gamma} t + \Delta t) + f_i(\boldsymbol{X}_{\Gamma} t)]\boldsymbol{e}_i, \tag{12}$$

where Γ is the border surface and i represents all possible directions. So to calculate the drag force it must be considered the forces in the horizontal direction and the forces in the vertical direction to calculate the lift. Considering the equation above and the first two presented in this paper it is possible to obtain the drag and lift coefficient.

Related to the bounce back boundary condition commented above, it is a boundary condition that do not works perfectly, but it is very easy to apply and it allows to obtain quite satisfactory results (Sukop and Thorne, 2005). The bounce back boundary condition is important to satisfy the condition that the velocities at the walls must be zero (no-slip condition) and this is done just by considering that when a fluid particle collides with a solid boundary it maintains the magnitude of its velocity, but with opposite direction. Below there is an illustration of the application of this boundary condition (Chirila, 2010)

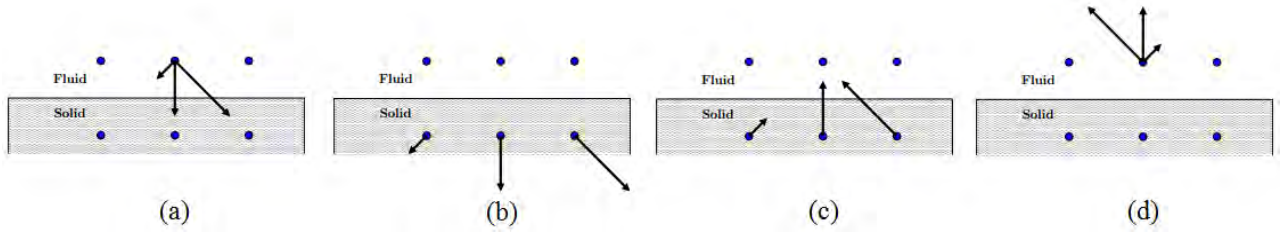

Figure 4. Illustration of the bounce back effect: (a) before stream t; (b) after stream; (c) after bounce back and (d) before stream t + Δt.

Another boundary condition considered for this paper is the one indicated by Hecht and Harting (2010), which involves the specification of the velocity or pressure locally on each lattice site. So, their values are independent of other simulation parameters. For the simulations considered in this paper, it was prescribed the velocity at the entrance of the channel and the pressure at the exit of the channel, just as it usually is in practical experiments. The application of this boundary condition is important for this kind of simulation because this way the value of the parameters of the channel's exit do not influence the values of the parameters of the channel's entrance. Moreover, using this boundary condition make it easy to specify the Reynolds number for a simulation as desired. The Fig. 5 illustrates the application of this boundary condition.

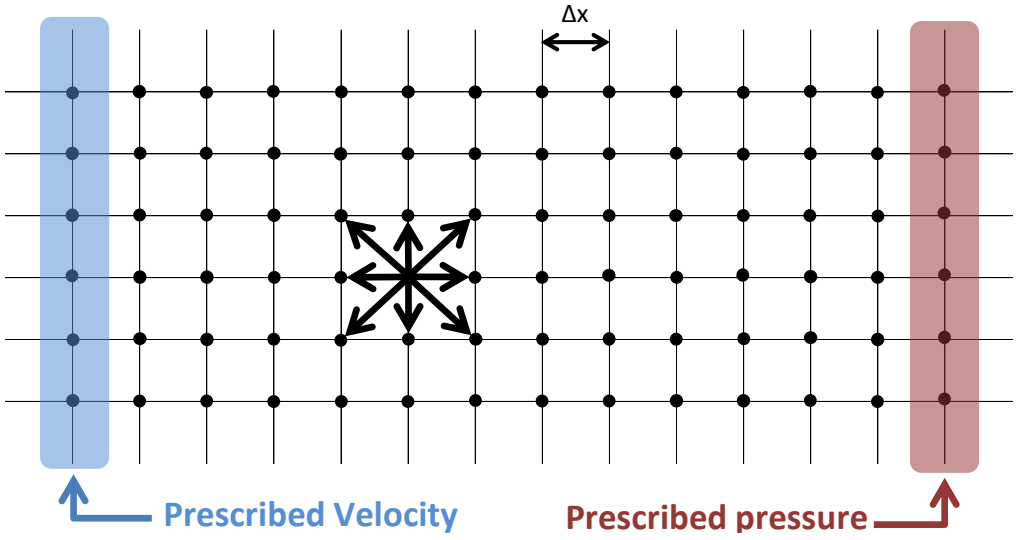

Figure 5. Illustration of on-site velocity and pressure boundary conditions for D2Q9 model.

ISSN 2176-5480

3. RESULTS AND DISCUSSION

For the simulations used to comparison of the Reynolds number with experimental results the following channel dimensions had been considered: 801x801; 1201x1201; 1601x1601; 2001x2001 and 2401x2401. The diameter of the cylinder was considered as been 66 lattice units as may be observed further in this paper it is possible to obtain accurate results using smaller cylinders and actually this has been considered for first simulations. However, it became a problem for the highest numbers of Reynolds considered in the simulations, as commented above there is a limitation of speed in the Lattice Boltzmann method due to compressible effects, so to obtain a Reynolds number of 75, for instance, it was needed to increase the diameter of the cylinder. Moreover, the D/L ratio would be very small keeping the initial channel dimensions, so they were increased too. So, the cylinder diameter has been increased to 66 lattice units and the channels dimensions to those shown above. Another solution would be decreasing the viscosity of the fluid. However it was decided to keep the same value.

The procedure to obtain the drag coefficient for different Reynolds number consisted in simulating a flow over a cylinder in different channel sizes and after that to plot ln C_D against 1/L, where L corresponds to the dimension that has been varied. Then, using a linear fitting curve the value of the ln C_D was obtained, considering that when L tends to infinity 1/L tends to zero, so the ln C_D value was the one that the linear fitting curve intercepts the vertical axis.

It is very important to compare the results obtained to experimental results or some good approximations presented in the literature. So, the results were compared to Tritton (1959) experiments which estimates a mean curve based on experimental observations and also by using the equations developed by Clift et al. (1978). The approximated equations of experimental results presented by Clift et al. (1978) are shown in Tab. 1:

Table 1. Equations for determining drag coefficient.

Equation	Reynolds
$C_D = C_D'(1 + 1{,}147Re^{0{,}82})$	$0{,}1 < Re \leq 5$
$C_D = C_D'(1 + 0{,}227Re^{0{,}55})$	$5 < Re \leq 40$
$C_D = C_D'(1 + 0{,}0838Re^{0{,}82})$	$40 < Re \leq 400$

where $C_D' = 9{,}689Re^{-0{,}78}$.

3.1 Effect of cylinder diameter (Re = 1)

It has been evaluated the influence of the cylinder diameter in the drag coefficient values. For this analysis two different boundary conditions has been tested, one is the same already commented which is the prescription of the velocity at channel's entrance and of the pressure at the channel's exit. The other one is the prescription of the velocity all over the borders of the channel. For both cases the ratio L/D was kept constant. It has been noted that for the two boundary conditions considered the diameters above 15 lattice units there is no significant variation in the results as shown in Fig. 6a.

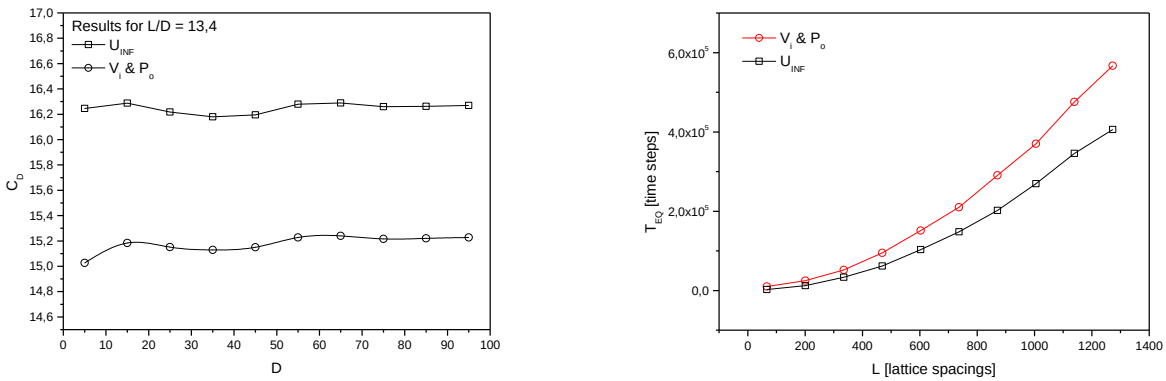

(a) (b)

Figure 6. Calculation of the drag coefficient under different resolutions and boundary conditions. In (a) it is shown the effect of the cylinder diameter, keeping the ratio L/D constant for Re = 1. The graph (b) exhibits how long it is necessary to reach steady state conditions for different domain sizes $L \times L$.

ISSN 2176-5480

3.2 Effect of domain size (Re = 1)

Comparing the convergence value using two different diameters, 15 and 33 lattice units, and considering the same boundary conditions commented in the last subtopic. As shown in Fig. 7 it may be noted that for this case also there is no significant difference in the results using different diameters once they are above 15 lattice units.

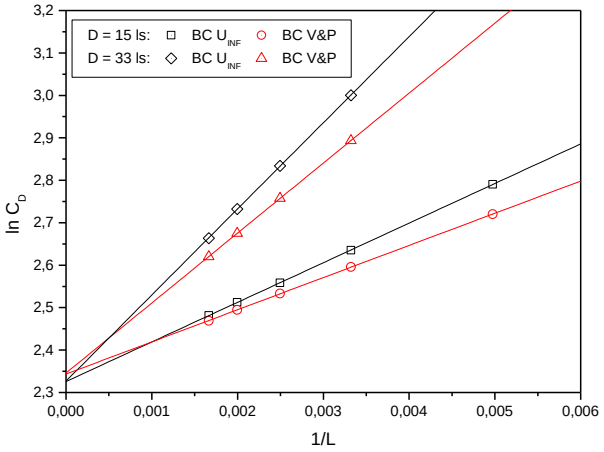

Figure 7. Effect of the simulation domain size on the calculation of the drag coefficient. It is shown that C_D depends strongly on the domain size $L \times L$.

3.3 Comparison with experimental results for different Re

So, applying the procedure described in topic 3 it has been obtained the results presented in the sequence:

For Reynolds number equal to10, observing the Fig. 8 and Tab. 2 it can be noted that in fact there is a linear tendency between $\ln C_D$ and 1/L so that it can be used to approximate the drag coefficient value to the one corresponding to an infinity domain. The value obtained for Reynolds number equal to 10 is not so close to the literature as expected, however, the values of the drag coefficient according to Clift et al. (1978) and Tritton (1959) also present a considerable difference between each other for this Reynolds number.

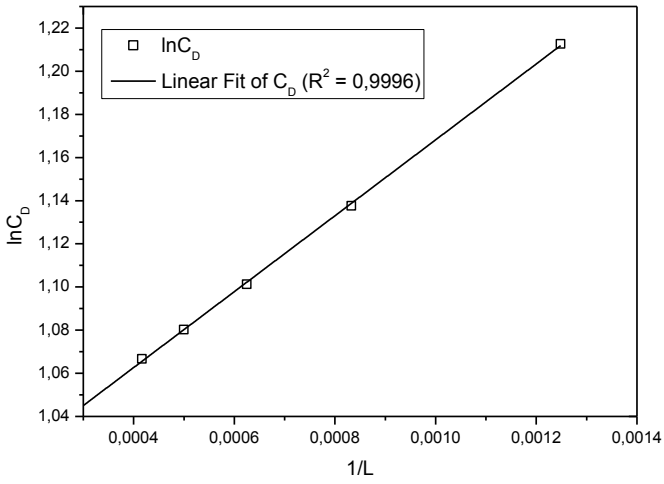

Figure 8. Simulation result of drag coefficient for Re = 10.

The value of ln C_D when the linear fit line intercepts the vertical axis is 0,9922, so $C_D = 2{,}6972$.

Table 2. Comparison of the result obtained from simulation with the literature for Re = 10.

C_D LBM	Tritton (1959)	Clift et al. (1978)	Error - Tritton (1959)	Error – Clift et al. (1978)
2,6972	2,9460	3,1883	8,4%	15%

ISSN 2176-5480

Figure 9 illustrates the streamlines of the flow over the cylinder, this image was obtained from the simulation of the domain 1601x1601, actually it is just part of the domain to better illustrate the streamlines.

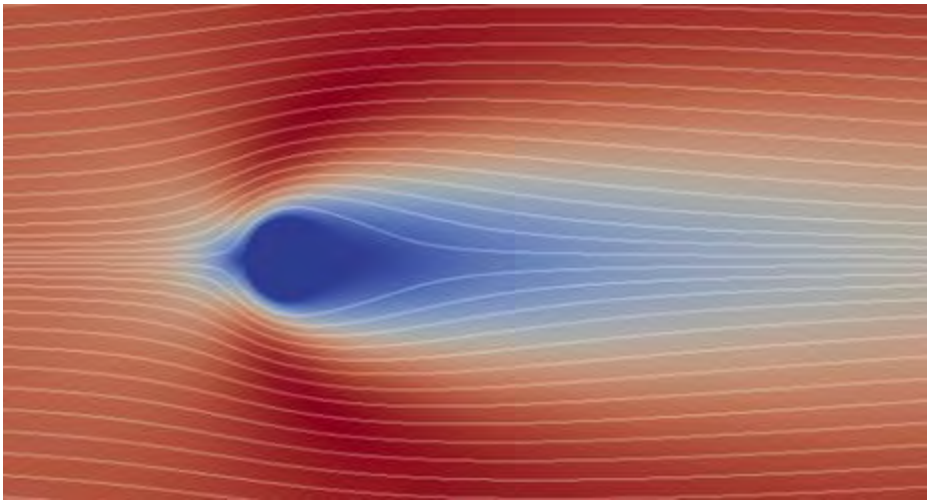

Figure 9. Result of the simulation of the flow over a cylinder for Re = 10 and domain 1601x1601.

Considering Reynolds number equal to 50 the results with the simulations is very close to the values of the literature as shown in Tab. 3. However, do not exist a linear tendency between $\ln C_D$ and 1/L considering the domain dimensions simulated as may be seen in Fig. 10, the R-Square value of this linear fit of $\ln C_D$ is just 0,7580 which shows this statement.

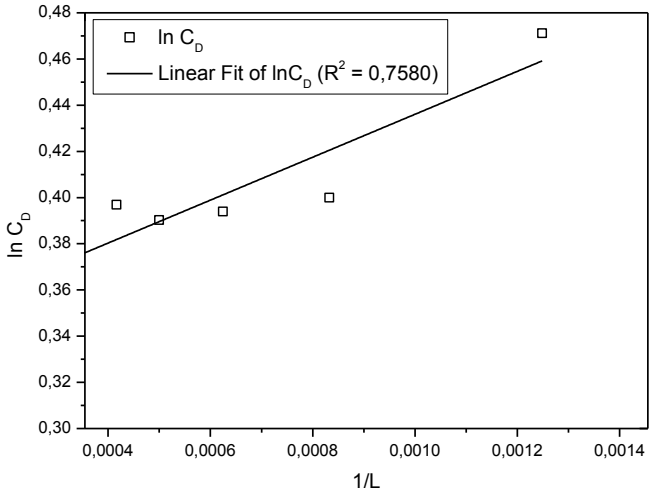

Figure 10. Simulation result of drag coefficient for Re = 50.

The value of ln C_D when the linear fit line intercepts the vertical axis is 0,34312, so $C_D = 1,4093$.

Table 3. Comparison of the result obtained from simulation with the literature for Re = 50.

C_D LBM	Tritton (1959)	Clift et al. (1978)	Error - Tritton (1959)	Error – Clift et al. (1978)
1,4093	1,4598	1,4077	3,46%	0,11%

The reason why the results of Reynolds number equal to 50 do not have a linear behavior is probably because of Reynolds number around 50 is needed bigger domains to the development of the vortex shedding behind the cylinder and so obtain more accurate values of drag coefficient, this situation it is shown by Fig. 11 and Fig. 12. The first one is part of the domain 801x801 which illustrates just a circulation right behind the cylinder. However, there is no vortex shedding behind it as it should be. The second one is part of the domain 2401x2401 which shows the vortex shedding.

ISSN 2176-5480

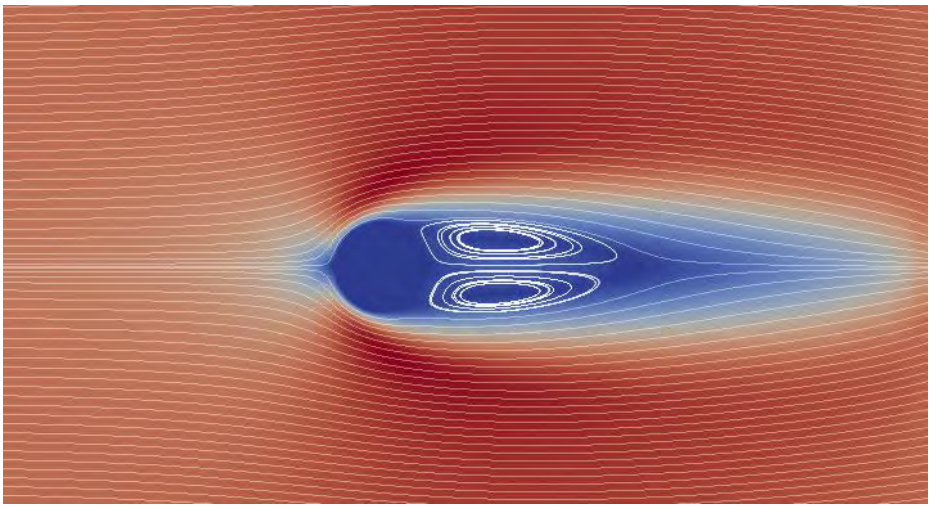

Figure 11. Result of the simulation of the flow over a cylinder for Re=50 and domain 801x801.

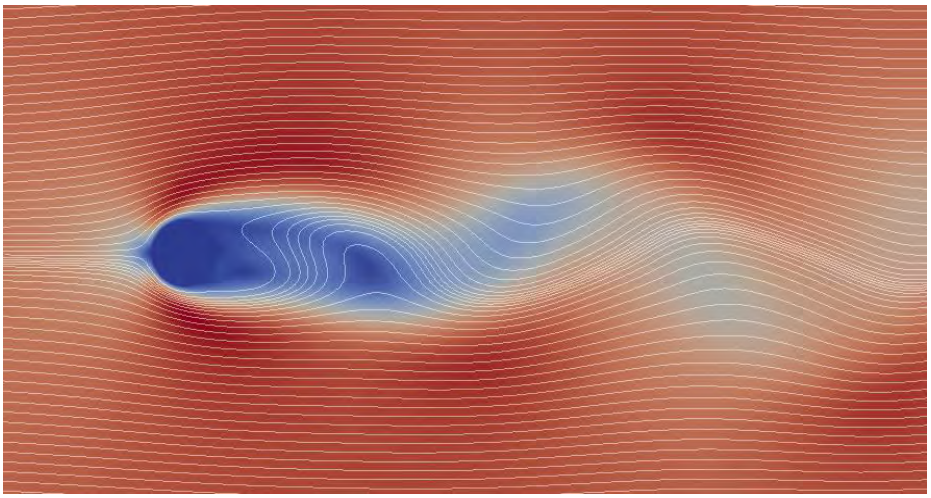

Figure 12. Result of the simulation of the flow over a cylinder for Re=50 and domain 2401x2401.

The results for Re = 75 can be considered as been good, the Tab. 4 shows the comparison between the literature values of drag coefficient for this Reynolds number and the one obtained from simulation. The linear fitting curve may be seen as a good approximation for the results of the simulations for Re = 50, the Fig. 13 shows it.

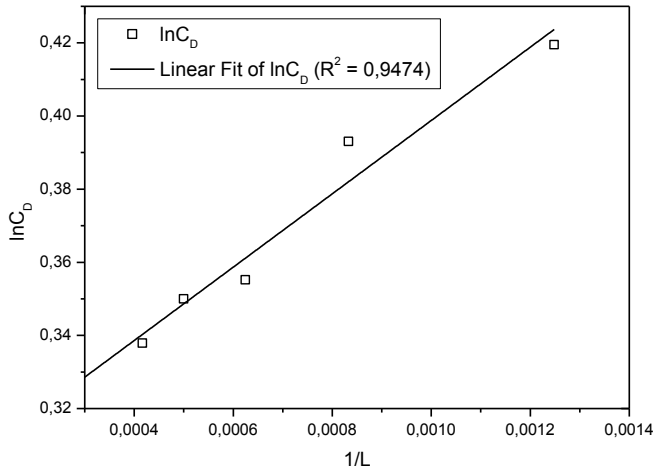

Figure 13. Simulation result of drag coefficient for Re = 75.

ISSN 2176-5480

The value of ln C_D when the linear fit line intercepts the vertical axis is 0,29855, so $C_D = 1,3479$.

Table 4. Comparison of the result obtained from simulation with the literature for Re = 75.

C_D LBM	Tritton (1959)	Clift et al. (1978)	Error - Tritton (1959)	Error – Clift et al. (1978)
1,3479	1,3445	1,2990	0,3%	4%

The appearance of the flow over a cylinder for Reynolds number equal to 75 according the simulation of a domain 1601x1601 is as demonstrated in Fig. 14 where is possible to see the vortex formation behind the cylinder which do not need so much space to be completed formed as it is needed in the case of Re = 50.

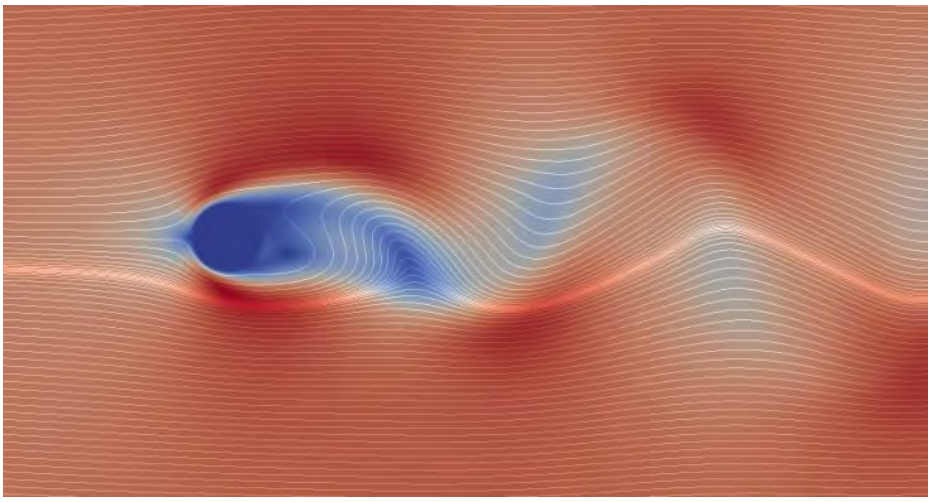

Figure 14. Result of the simulation of the flow over a cylinder for Re = 75 and domain 1601x1601.

For Reynolds number equal to 100, the drag coefficient value obtained is pretty similar with the one presented in the literature as presented in Tab. 5 and in fact there is a linear tendency between the results of the simulations done as illustrated in Fig. 15.

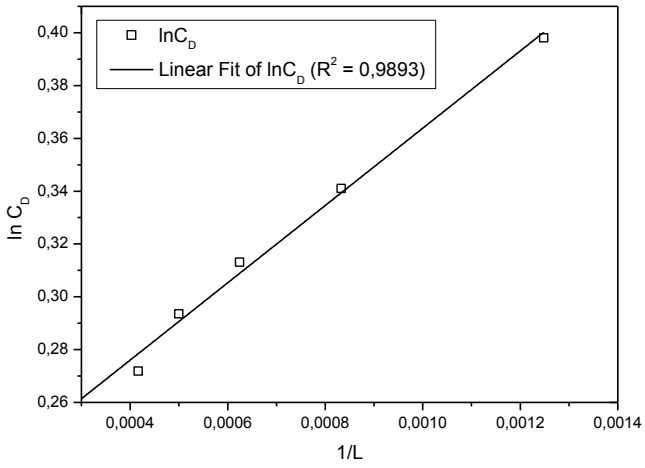

Figure 15. Simulation result of drag coefficient for Re = 100.

The value of ln C_D when the linear fit line intercepts the vertical axis is 0,21749, so $C_D = 1,2430$.

Table 5. Comparison of the result obtained from simulation with the literature for Re = 100.

C_D LBM	Tritton (1959)	Clift et al. (1978)	Error - Tritton (1959)	Error – Clift et al. (1978)
1,2430	1,2798	1,2430	2,9%	0%

ISSN 2176-5480

For Reynolds number = 100 the appearance of the flow pattern is very similar to the one for Re = 75. The Fig. 16 demonstrates it. This figure is part of the image generated for a domain size of 2001x2001.

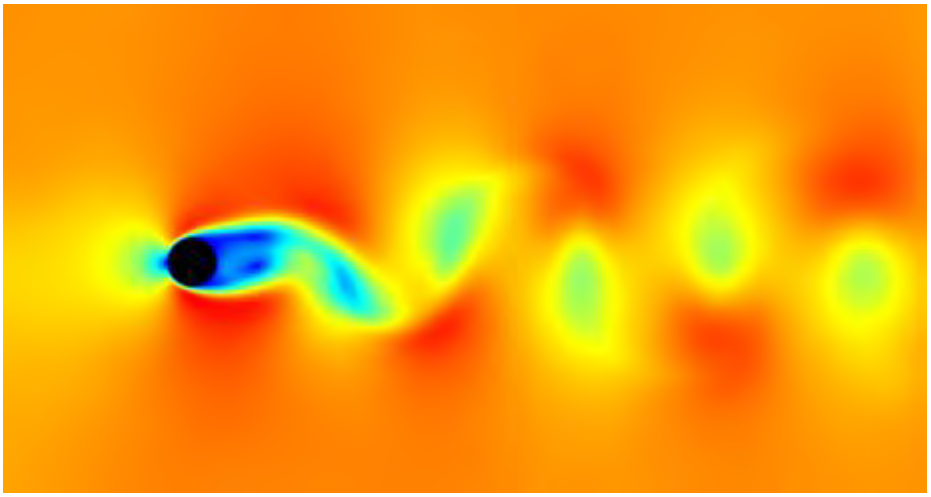

Figure 16. Result of the simulation of the flow over a cylinder for Re = 100 and domain 2001x2001.

4. CONCLUSION

First of all, it is easy to figure out the importance of the domain size for determining the drag coefficient by observing the results of this work. In addition, it is essential to note the influence of the number of different dimensions analyzed. For example, in the case where Re = 50, it is easy to see that one less point evaluated can make a significant difference in the results, although the result obtained is a good approximation to the literature and actually that case the results can not properly be related with their selves by a linear curve.

The overall results were consistent. Using the Lattice Boltzmann method in combination with the technique presented above can lead to some very good approximations of drag coefficient values. The major error observed for predicting the drag coefficient was for Reynolds equal to 10, an error of 15 % according to Clift et al. (1978) and 8,4 % considering Tritton (1959). However, for this Reynolds number it is observed a strong linear trend between the $\ln C_D$ and 1/L values. On the other hand, for Reynolds number equal to 50 it is not observed a linear trend among the results of the simulations done, this method of determining the drag coefficient should be better studied for this case. Even though, the result obtained for this Reynolds number was similar with both Clift et al. (1978) and Tritton (1959) results, principally the former. For other Reynolds values considered in the analyses, in fact it was observed good accuracy in the results for the determination of drag coefficient with a well linear tendency observed from the simulation results.

In the future, it is possible to analyze the ideals D/L ratios for this kind of analysis and also verify the number of points that should be considered for better accuracy in the results.

5. REFERENCES

CHEN, H.; CHEN, S.; MATTHAEUS, W. H., 1992. *Recovery of the Navier-Stokes equations using a lattice-gas Boltzmann method*. Physical Review A, 45(8):R5339-R5342.

CHIRILA, Dragos B., 2010. “Introduction to Lattice Boltzmann Methods”. 01 Jun. 2013 <http://www.awi.de/fileadmin/user_upload/Research/Research_Divisions/Climate_Sciences/Paleoclimate_Dynamics/Modelling/Lessons/Einf_Ozeanographie/lecture_19_Jan_2010.pdf>

CLIFT, Roland; GRACE, J. R.; WEBER, M. E., 1978. *Bubles Drops, and Particles*. New York: Academic Press, 380p.

DEVENPORT, William J.. ”Flow Past a Circular Cylinder”. 04 May. 2013 <web.iitd.ac.in/~pmvs/mel705/cylinder.doc>

FRISCH, U.; HASSLACHER, B.; POMEAU,Y., 1986. *Lattice-gas automata for the navier-stokes equations*. Physical Review Letters, 56(14):15051508.

HECHT, M.; HARTING, J.D.R., 2010. *Implementation of on-site velocity boundary conditions for D3Q19 lattice Boltzmann. Journal of Statistical Mechanics : Theory and Experiment*.

HOMANN, F.; ANGEW, Z., 1936. Math. .Mech. 16, 153-164.

HOUGHTON, Edward Lewis; CARPENTER, Peter William, 2003. Aerodynamics for Engineering Students. Oxford: Butterworth Heinemann, 5th edition.

NASA, Nacional Aeronautics And Space Administration. “Flow Past a Cylinder”. 04 May. 2013 <http://www.grc.nasa.gov/WWW/k-12/airplane/dragsphere.html>.

QUIAN, Y. H.; HUMIÈRES, D. d'; LALLEMAND, P., 1992. *Lattice BGK models for Navier-Stokes equations. Europhysics Letters*, 17(6):479-484.

ROTHMAN, D. H.; ZALESKI, S., 1997. *Lattice-Gas Cellular Automata - Simple Models of Complex Hydrodynamics*. Cambridge University Press, Cambridge.

SUKOP, Michael C.; THORNE, Daniel T. Jr, 2005. *Lattice-Boltzmann Modeling: An Introduction for Geoscientists and Engineers*, Springer-Verlag Miami, LLC.

SURMAS, R.; SANTOS, L.O.E. dos; PHILIPPI, P.C., 2004. *Lattice Boltzmann simulation of the flow interference in bluff body wakes*, Future Generation Computer Systems, 20 (6): 951-958.

TRITTON, D. J.,1959. "*Experiments on the flow past a circular cylinder at low Reynolds numbers*". Cambridge.

WOLF, Fabiano G., 2006. *Modelagem da Interação Fluido-sólido para Simulação de Molhabilidade e Capilaridade Usando o Modelo Lattice-Boltzmann*. 2006. 154 p. Doctoral thesis, Federal University of Santa Catarina, Florianópolis.

WOLFRAM, S., 1986. *Cellular automaton fluids 1: Basic theory*. Journal of Statistical Physics, 45(3/4):471526.

6. RESPONSIBILITY NOTICE

The author(s) is (are) the only responsible for the printed material included in this paper.